Proceedings of ICRC 2001: 581 © Copernicus Gesellschaft 2001

ICRC 2001

Tunka EAS Cherenkov Array – status 2001

N. Budnev[2], D. Chernov[1], V. Galkin[1], O. Gress[2], T. Gress[2], E. Korosteleva[1], L. Kuzmichev[1], B. Lubsandorzhiev[3], A. Panfilov[3], V. Pan'kov[2], Y. Parfenov[2], P. Pokhil[3], V. Prosin[1], Y. Semeney[2], Ch. Spiering[4], T. Schmidt[4], R. Vasiliev[3], and I. Yashin[1]

[1]Skobeltsyn Institute of Nuclear Physics MSU, Moscow, Russia
[2]Irkutsk State University, Irkutsk,Russia
[3]Institute for Nuclear Research, Moscow, Russia
[4]DESY–Zeuthen, Zeuthen, Germany

Abstract. The EAS Cherenkov array TUNKA has been extended significantly in October 2000. It consists now of 25 wide angle integral detectors of Cherenkov light flux based upon the QUASAR–370 PMT and 4 detectors of light pulse shape using Thorn-EMI D668 PMT of 20 cm diameter and cone reflectors. The detectors are deployed in the square of 340x340 m^2.

1 Introduction

Several years ago three groups of our collaboration have begun the construction of TUNKA Cherenkov EAS array in Tunka Valley, 50 km to the west from the Lake Baikal(51.49 N, 103.04 E, at 680 m above sea level). Its purpose is the study of the energy spectrum and the chemical composition of cosmic rays in the region of the "knee" ($3 \cdot 10^{15}$ eV). The changes of the spectrum and composition in this region can play the key role in understanding of the Galactic cosmic rays origin. The method of EAS Cherenkov light recording using the atmosphere of Earth as a huge calorimeter seems to be the most adequate one to study the very high energy primary cosmic rays.

TUNKA–13 array started data acquisition in 1996. It consisted of 13 phototubes (PMs) QUASAR–370 (Bagduev et al., 1999) with 37 cm diameter photocathode, arranged within a square of 240 m side. The results of study of energy spectrum and chemical composition with this array may be found in our previous publications (Gress et al., 1997: Gress et al., 1999.). The TUNKA – 13 data clearly show the existence of the "knee" in the energy spectrum of primary cosmic rays at the energy 3 – 4 PeV and some irregularities below and above the "knee" which could be explained in the spirit of Erlykin–Wolfendale model (Erlykin and Wolfendale, 1997)

Together with Tunka experiment we installed 5 our Cherenkov light detectors in Gran Sasso for common work with EAS-TOP array to cross-check our algorithm of determination of EAS parameters.

Correspondence to: L. Kuzmichev (kuz@dec1.sinp.msu.ru)

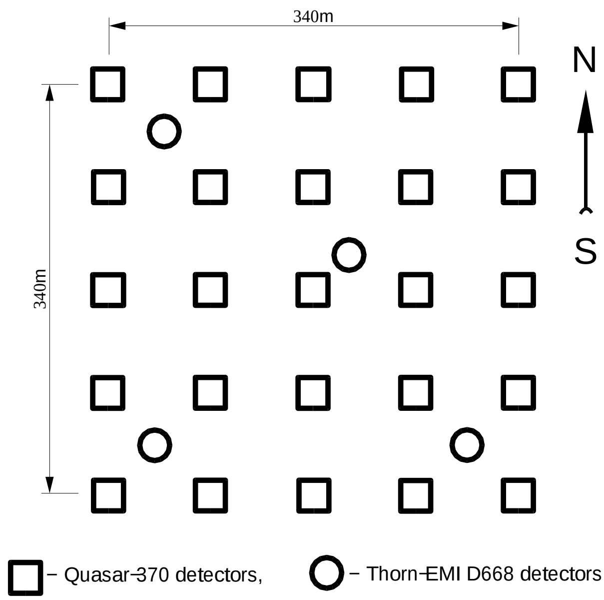

Fig. 1. Schematic view of the Tunka EAS Cherenkov array

The array was essentially modified in 2000(Fig.1.) The number of detectors, based upon QUASAR–370, was increased to 25. We added four detectors of Cherenkov light pulse shape. All detectors were placed in the square of 340 m side. The enlargement of the array area will let us get more statistics with high energy resolution at the energy range 10 – 100 PeV, where the additional changes of the spectrum and composition are expected.

2 Description of the array

Detectors, based upon QUASAR–370 were described in detail in our early publication (Brynski et al., 1995). The QUASAR–370 is a hybrid phototube which consists of an electro–optical preamplifier with a hemispherical photocathode, followed by

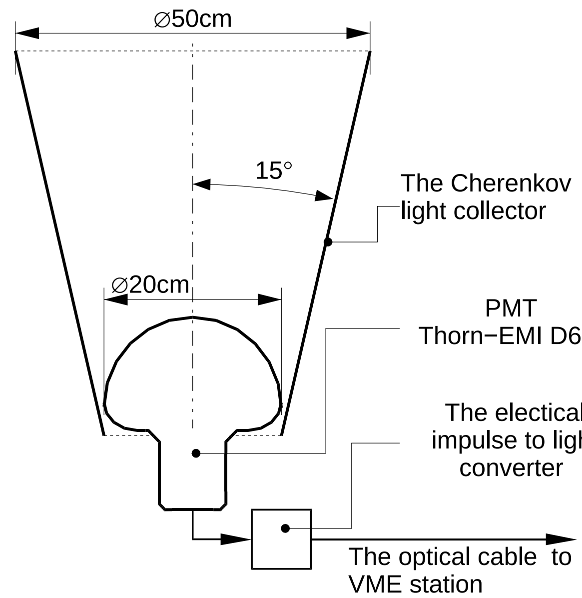

Fig. 2. Cherenkov signal waveform detector.

a small conventional PM with 2.5 cm photocathode. In order to decrease the output DC current due to light background from the night sky, we use only 5 stage of PM. The overall gain of the phototube is about 10^4. This low gain is compensated by a low noise preamlifier connected directly to the 6th dynode of the PM. In addition to the phototube itself, each detector contains HV supplies (20 kV and for the electro–optical preamplifier and 1 kV for the small PM.), preamplifier (with gain 10) and a calibration LED. The detector aperture is about 30 degrees half angle. Signal from the preamplifier are led to the central electronic station by the coaxial cables. This station consists of the amplifiers, CF discriminators, 12–bit TDCs with 0.5 ns step, 13–bit ADCs with 100 ns individual for each channel gates and a trigger system. The trigger condition is ≥ 4 hit in any 25 detectors within a 1 μsec gate. The hardware threshold is set to about 150 photo-electrons. The amplitude measurement is linear up to 10^5 photo-electrons. The relatively large effective area of QUASAR tube and wide dynamic range of amplitude measurements allows to study the energy spectrum from less than 0.5 PeV up to 100 PeV.

The decay time of scintillator, used in QUASAR electro – optical preamplifier is about 40 ns and so it is practically impossible to use this tube for the measurement of light pulse shape, so for this purpose in a new detectors we use fast 6–stage hemispherical PMs (Thorn–EMI D668) (Fig. 2). This phototube has been developed by EMI for the AIROBICC Cherenkov array (Karle et al., 1995). Using of cone reflectors the effective area of the optical sensor is increased the effective area of the detector to nearly 0.2 m^2 for vertical direction. Analog signals from PMs, after amplification with gain 10, is transmitted to the central electronic station by optical fiber cables. This method has been developed by DESY group for AMANDA Neutrino Telescope (Karle et al., 1997) With this method we avoid any relevant distortion of the signal, even after 250m cable. In central electronics hut the signals are digitized by two 8–bit FADC (DL515) with 2 ns resolution. The conversion of signals begins when the signal amplitude in one of PMs exceeds electronic threshold, in a case of QUASAR detector trigger takes place, the data from FADC buffers is written to computer. The sensitivity of shape detectors gives the possibility to measure pulses shape at the distance more than 200 m (what is interesting from physical point of view) for showers with energy more than 2 PeV.

3 Experimental data processing

The EAS parameters reconstruction procedure is almost the same as it has been for TUNKA – 13 (Gress et al., 1999). The base EAS parameters are zenith and azimuth angles, shower core location, individual lateral distribution function slope parameter R_0 and the photon density at a fixed distance 100 m from the core Q_{100}. To derive Q_{100} and R_0 we use the readings of the detectors in the range of core distances from 20 to 150 m only, because Monte-Carlo simulation shows (see below), that this range is the most sensitive to the EAS longitudinal development.

The experimental estimates of the main parameters accuracy have been made by comparison of EAS parameters derived at EAS-TOP using independently Cherenkov data and data of scintillators for the same event. The accuracy of space angle has been less than 0.5^0. The accuracy of core location is less than 7 m and the accuracy of parameter R_0 determination is better than 5 m, accuracy of Q_{100} determination is better than 10%.

The pulse duration at the half maximum level $\tau_{1/2}$ is the most accurately measured parameter of the shape, as it has been shown at previous works (Kalmykov et al., 1975). So we use the same parameter to make the quantitative analysis of the data.

To derive A_{max} and $\tau_{1/2}$ from the measured experimental points we use the following approximation (previously tested with simulated pulses) with three independent parameters a, b and c:

$$A(t) = a(1 - exp[-(\frac{t-b}{c})^2]) \cdot exp - (\frac{t-b}{c}) \qquad (1)$$

The example of recorded pulse and fit with this expression is shown at Fig. 3.

To get the correct value of $\tau_{1/2}$ we must take into account the response function of PMT and recording apparatus. This problem has been solved by convolution of the response function and input pulse, and then deriving the dependence of output pulse parameter $\tau_{1/2}$ on input pulse parameter. To find the response function we should find the reaction of the system on the light pulse with the time duration much smaller than the time resolution of the system. We use light pulses from EAS at the distances 50 – 100 m from the core as the shortest ones ($\tau_{1/2} \sim 2ns$). The best fit of response function $F(t)$ is as follows :

$$F(t) = C \cdot (t/\tau_0)^\alpha \cdot e^{-t/\tau_0}, \tag{2}$$

where $\alpha = 2.85$, $\tau_0 = 2.1$ ns. Using the procedure, described above, we have derived the following expression for recalculation from measured $\tau_{1/2m}$ to the original one $\tau_{1/2r}$ (all in ns):

$$\tau_{1/2r} = \sqrt{\tau^2_{1/2m} - \tau^2_{1/2a}} - 2.2, \tag{3}$$

here $\tau_{1/2a} = 7.4$ ns. This expression is a good fit of calculated points for $\tau_{1/2m}$ from 7.8 ns to about 40 ns.

4 Monte Carlo Simulations

EAS events were simulated using the CORSIKA code with the QGSJET options. Cherenkov light lateral distribution function (LDF) have been obtained for each event inside the core distances from 2.5 to 400 m with the step 5 m. Cherenkov light pulse shape has been obtained for the same fixed distances with the step 2 ns. Primary proton and iron showers were produced for 3 different energies: 1.0, 2.0 and 5.0 PeV - and 2 zenith angles: 0^o and 30^o. The whole number of 90 independent simulated events has been analyzed by now (48 for 1 PeV, 30 for 2 PeV and 12 for 5 PeV). The acquisition of simulated events is being continued now.

To analyze the sensitivity of EAS parameters to the longitudinal development we combine three parameters – the total vertical depth of the atmosphere X_0, depth of shower maximum development X_{max} and zenith angle of the shower θ – to one $\Delta X = X_0/cos\theta - X_{max}$. The connections between different parameters for different energies were found to be the same inside the energy range under analysis. So to examine the connection between Q_{100} and ΔX we use all the simulated energies with simple proportional correction of Q_{100}.

5 Approach to the mass composition

The approach to the mass composition is based upon the fact that the different nuclei produces showers with the different mean depth of maximum. To measure the depth of EAS development maximum one can use such observable features of EAS as the shape of Cherenkov light LDF and the shape of Cherenkov light pulse.

5.1 Analysis of LDF

If the linear scale is used for x-axis and logarithm scale is used for the y-axis then the simulated LDF can be described with the following main features:

1) There is almost liner part from about 20 m to about 150 m from the axis. The slope of this part is the most sensitive to the longitudinal development of the individual event. So we can approximate LDF in this distance range as:

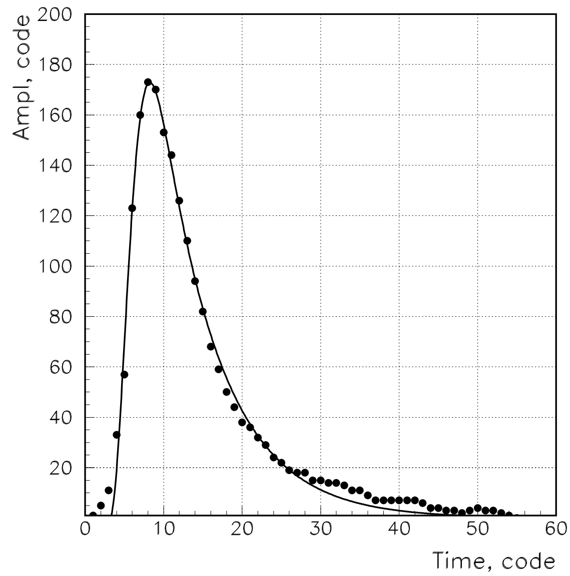

Fig. 3. Example of signal waveform. A unit of a time code is 2 ns. Curve - approximation using expression (1)

$Q(R) = Q_{100} \cdot exp((100 - R)/R_0)$ - with the variable parameters R_0 and Q_{100}.

2) The light flux increases rapidly closer to the axis.

3) At the distance range 150 - 200 m the slope of the LDF is almost independent on the individual longitudinal development of EAS.

The best fit of connection between R_0 and ΔX is:

$$log_{10}R_0 = a_0 + a_1\Delta X + a_2\Delta X^2. \tag{4}$$

Here a_n for protons is (1.754, -0.111$\cdot 10^{-2}$, 0.356$\cdot 10^{-5}$), and a_n for iron is (1.215, 0.117$\cdot 10^{-2}$, 0.915$\cdot 10^{-6}$). The residual standard deviation of individual simulated points from the approximation is less than 10% for vertical events and about 24% for $\theta = 30^o$.

5.2 Pulse shape analysis

The $log_{10}(\tau_{1/2})$ dependence on ΔX has a very interesting and essential feature that all the points for any sort of nuclei, energy and zenith angle can be fitted with one the same line for fixed core distance:

$$log_{10}(\tau_{1/2}) = C(R) \cdot \Delta X + D(R) \tag{5}$$

This is shown at fig.4 for core distances 200, 250 and 300 m. The residual standard deviation for all the simulated points and all the distances in the range from 200 to 400 m is about 3%. So the parameter $\tau_{1/2}$ is the best measure of longitudinal development from the theoretical point of view. Fig.5 shows the simulated energy dependence of R_0 and $\tau_{1/2}$ for primary proton and iron.

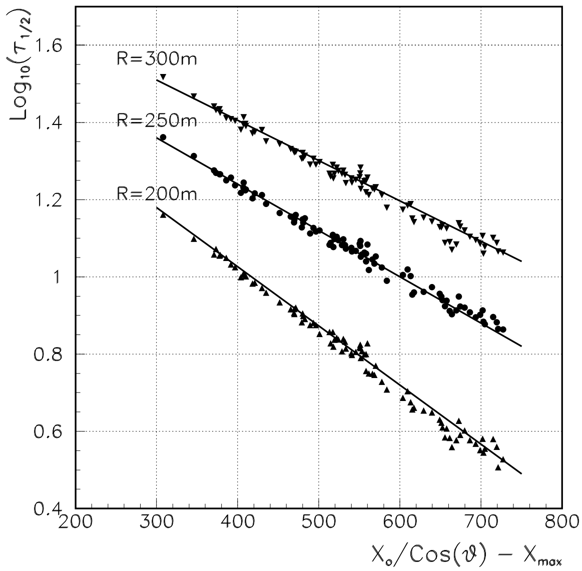

Fig. 4. The dependences of $\tau_{1/2}$ on $X_0/\cos(\theta) - X_{max}$ for different distances from the core. X_0 – total depth of the atmosphere, X_{max} – depth of the shower maximum.

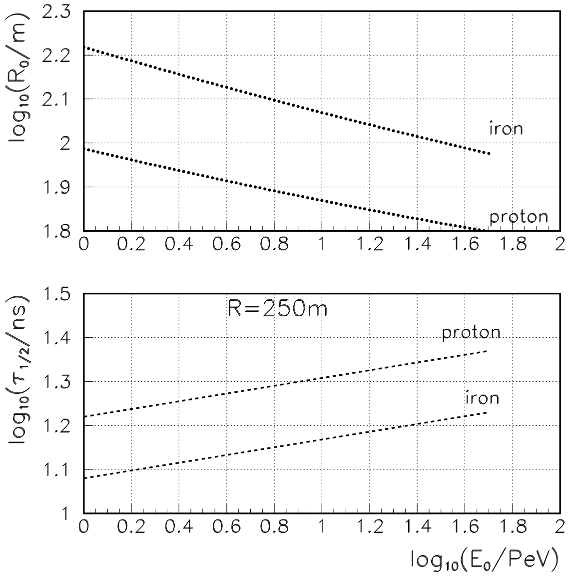

Fig. 5. The dependences of mean values of R_0 and $\tau_{1/2}$ for p and Fe on the energy .

6 Approach to the determination of energy

To derive the primary energy from the measured parameter Q_{100} we need to make correction of it's dependence on the longitudinal development of EAS.

The best fit of Q_{100} on ΔX dependence is:

$$log_{10}Q_{100} = log_{10}(E_0/PeV) + b_0 + b_1\Delta X + b_2\Delta X^2. \quad (6)$$

Here b_n is (0.812, 0.147$\cdot 10^{-2}$, -0.241$\cdot 10^{-5}$) for proton and b_n is (1.162, -0.144$\cdot 10^{-3}$, -0.999$\cdot 10^{-6}$) for iron. The residual standard deviation is about 5% for mono-nucleus composition and 17% for the mixture of protons and iron. Absolute shift of the curves for proton and iron is about 0.1 in logarithmic scale.

The common expression 5 can be approximated with line dependence in the limited range of zenith angles ($\theta \leq 25^o$), and thus give the practical expression:

$$log_{10}(E_0/PeV) = A \cdot \log_{10} Q_{100} + B \cdot (\sec\theta - 1) + C, \quad (7)$$

For mean unchangeable composition coefficients are: A=0.95, B=.65, C=2.12. It should be mentioned, that C=2.07 for proton and C=2.17 for primary iron. Simulation of apparatus response gives inaccuracy of this method of about 15% for single nucleus composition an about 30% for complex composition.

The more accurate method of recalculation can be combination of equations 5 and 6. ΔX is to be derived from $\tau_{1/2}$ and then inserted to the expression 2. This method can give the whole accuracy of energy about 20%. It has the only disadvantage for the existing array, because the detectors of pulse shape can control not the whole area (the detector-core distance has to be more than 200 m) and not the whole solid angle of the array.

7 Conclusion

The first winter season of operation of the new array is finished. The experimental data are presently analyzed. We plan to increase the number of detectors of pulse shape, based on EMI PMs and also to install two pulse shape detectors with 1 m diameter at the distance 400 m from the array center.

Acknowledgements. We would like to express our gratitude to Prof. G. Navarra from Torino University for the possibility of making the experiment with QUASAR phototubes at Gran Sasso and useful discussion, and to Dr. E. Lorenz from MPI Munich for his help with EMI phototube. This work was supported by the Russian Fund of Basic Research (grants 99-02-16892 and 98-02-04115), DFG – 486(RUS) 113/492, INTAS 96 –0526, and by the Russian Federal Program "Integration"(project A0-116).

References

Bagduev,R. et al., *Nucl. Instr. Meth.* **A420** P. 138, 1999.

Gress,O et al., Proc. of 25th ICRC V.4. P.129 – 132, 1997 (Durban)

Gress,O. et al., *Nucl. Physics B (Proc.Suppl.)* **75A** P.299 –301, 1999.

Erlykin,A. and Wolfendale,A. *Astropart. Phys.* **7** P.1, 1997.

Bryanski,S et al., Proc. of 24th ICRC V.2. P.724 – 727, 1995 (Roma)

Karle,A. et al,, *Astropart. Phys.* **3** P.263, 1995.

Karle,A. et al., *Nucl. Instr. Meth.* **A287** P. 274, 1997.

Kalmykov, N et al., Proc. 14th ICRC, V8. P.3034,1975. Munich